EUROPHYSICS LETTERS 1 March 1997

Europhys. Lett., **37** (7), pp. 465-470 (1997)

Fe structural and magnetic phases in $Fe/Ni_{81}Fe_{19}(001)$ multilayers

W. Kuch(*) and S. S. P. Parkin

IBM Research Division, Almaden Research Center
650 Harry Road, San Jose, CA 95120, USA

(received 24 October 1996; accepted in final form 24 January 1997)

PACS. 61.10−i – X-ray diffraction and scattering.
PACS. 68.65+g – Low-dimensional structures (superlattices, quantum well structures, multilayers): structure, and nonelectronic properties.
PACS. 75.70−i – Magnetic films and multilayers.

Abstract. – The structure of epitaxially sputtered single-crystalline $Fe/Ni_{81}Fe_{19}(001)$ multilayers was studied using X-ray diffraction. As the thickness of the Fe layers is increased the structure of the Fe layers changes from vertically expanded fcc (001) to relaxed fcc (001), and finally, to bcc (011), thus identically replicating the structural behavior found in thin Fe films on Cu(001) single crystals. Corresponding to the structural transitions of the Fe layers are changes in the magnetic properties. The relaxed fcc phase contains non-magnetic Fe, which can lead to antiferromagnetic coupling of the $Ni_{81}Fe_{19}$ layers across the Fe layers.

The structure and magnetic properties of magnetic multilayers have attracted increased attention in recent years. This is because of interest both in understanding the fundaments of the novel magnetic phenomena they exhibit and in their potential commercial importance for magnetic-field sensors for a variety of applications. These applications include magnetic recording read heads and non-volatile magnetic storage cells. A detailed understanding of the relationship between the structure and magnetism of ultra-thin films and multilayers will more readily allow the development of structures with magnetic properties tailored for particular applications.

Perhaps the most widely studied system to explore the correlation between structure and magnetism is that of thin epitaxial Fe films [1]-[7]. In this system a theoretically predicted dependence of the magnetic phase on the atomic volume of fcc Fe [8] has been confirmed experimentally. On Cu(001), the Fe films assume a vertically expanded fcc-like structure for thicknesses below 4 monolayers (ML) [1] and a relaxed fcc structure at thicknesses between 4 and 11 ML [2]. The smaller atomic volume of the relaxed structure is correlated with an antiferromagnetic phase of Fe [3], [4], whereas the expanded fcc structure, which has a higher

(*) On leave of absence from Max-Planck-Institut für Mikrostrukturphysik, Weinberg 2, D-06120 Halle, Germany.

atomic volume, exhibits ferromagnetism [3], [5]. Fe films thicker than 11 ML transform into the ferromagnetic bcc (011) phase [6], [7]. This richness in different structural and magnetic phases makes ultrathin Fe films a most interesting candidate also for studying coupling and transport phenomena. Up to now, however, these phases were only observed in single thin films.

In this paper we show that Fe layers in epitaxial Fe/$Ni_{81}Fe_{19}$(001) multilayers, prepared by Ar plasma dc-magnetron sputtering and subsequently exposed to air, exhibit a very close similarity to Fe/Cu(001). The sequence of three structural phases observed in Fe/Cu(001) as well as their associated magnetic behavior are all identified in the multilayers. This opens the possibility to explore the complex magnetic and structural properties of Fe as well as their interrelationships not only in ultrathin films but also in multilayered structures.

The multilayers were prepared by dc magnetron sputtering. MgO(001) was used as a substrate, on which Fe and Pt seed layers were grown at a temperature of ≈ 770 K. The multilayers were deposited at $T \approx 315$ K and capped with 30 Å Pt. The sample structures are MgO(001)/Fe(5 Å)/Pt(50 Å)/[$Ni_{81}Fe_{19}$(25 Å)/Fe(t_{Fe})]$_{12}$/Pt(30 Å), where t_{Fe} is the Fe layer thickness.

X-ray diffraction data were obtained under atmospheric pressure and at ambient temperature with a four-circle diffractometer with Cu-K_α radiation. In-plane lateral lattice constants were derived from off-specular 2Θ values of the (111) multilayer diffraction peaks and the specular (002) peak. The vertical lattice constant was determined from specular diffraction scans around the (002) reflection. To extract these values, a fitting routine developed by Fullerton and described in ref. [9] was employed to fit the experimental data. A simple multilayer model was used consisting of two independently strained layers with a common in-plane lattice constant. Neither interdiffusion, nor strain profiles within the individual layers, nor interface roughness were included. Instead, coherent scattering was assumed to be maintained over only a limited number of bilayers. The thickness of the permalloy layers was determined from a preliminary series of fits and then kept constant. The only free fitting parameters were the Fe layer thickness t_{Fe}, the vertical atomic-layer separation of each constituent layer, and the Gaussian width and average number of bilayers which scatter coherently. To account for the scattering from the Pt seed and capping layers, a Lorentzian of order n was fitted to each X-ray scan, where n ranged between 1.6 and 1.8. The accuracy in the determination of t_{Fe} is better than 0.2 Å.

With the exception of small Fe thicknesses ($t_{Fe} \leq 4$ Å), where the scattered intensity between two maxima is not completely reproduced in the calculation, this simple model yields good agreement with the experimental data. An example for $t_{Fe} = 8$ Å is shown in fig. 1. Further refinements of the model did not result in significant changes of the interlayer distances, and thus are not considered here.

The top panel of fig. 2 shows the Fe interlayer spacing d_{Fe} as a function of Fe layer thickness t_{Fe}. The resulting uncertainties in d_{Fe} are indicated by error bars. Two distinct regions of iron layer thickness can be distinguished from the Fe interlayer spacing: region I for t_{Fe} up to 6 Å, and region II for $t_{Fe} \geq 7$ Å. In the first region the Fe interlayer spacing varies between 1.85 Å and 1.88 Å with a maximum at $t_{Fe} = 5$ Å, whereas in the second region a slow decrease of the interlayer distance from 1.84 Å to 1.80 Å with increasing Fe layer thickness is observed. The in-plane lattice constant is approximately constant in region I, and increases slightly in region II from 3.552 Å at $t_{Fe} = 7$ Å to 3.563 Å at $t_{Fe} = 14$ Å. The iron is hence tetragonally expanded for all Fe thicknesses. The size of the distortion, *i.e.* the enhancement of the vertical as compared to the lateral lattice constant, is 5.9% at $t_{Fe} = 5$ Å, and relaxes from 3.6% at $t_{Fe} = 7$ Å to 1.4% at $t_{Fe} = 13$ Å. For constant atomic volume, the distortion in region II is equivalent to an in-plane strain of $\approx -1.2\%$ at $t_{Fe} = 7$ Å and $\approx -0.5\%$ at $t_{Fe} = 13$ Å. The relaxation of the Fe layer distortion in the second thickness range may be qualitatively

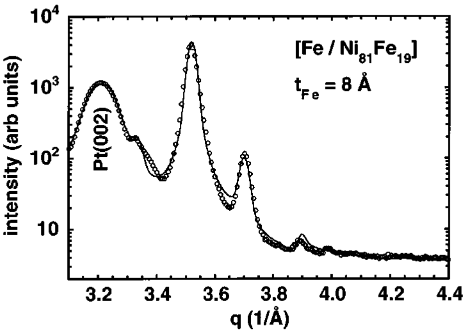

Fig. 1.

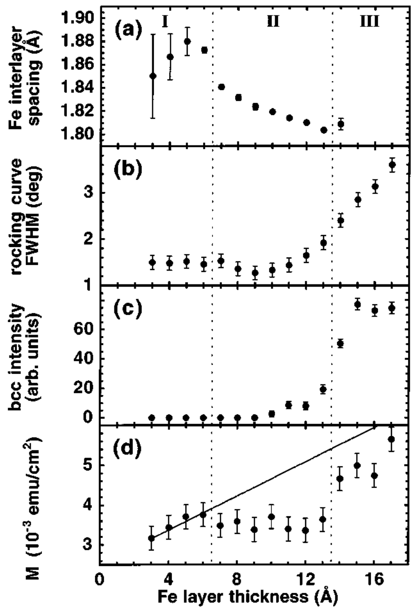

Fig. 2.

Fig. 1. – Specular X-ray diffraction scan around the (002) diffraction of a $[Ni_{81}Fe_{19}(25\ Å)/Fe(8\ Å)]_{12}$ multilayer. The contributions of the Pt seed and capping layers are indicated. The solid line represents the result of the fit as described in the text.

Fig. 2. – Structural and magnetic properties of the $Fe/Ni_{81}Fe_{19}$ multilayers as a function of the Fe layer thickness. (*a*) Atomic interlayer distance of the Fe layers. (*b*) Rocking curve full width at half-maximum of the fcc (002) multilayer specular diffraction spots. (*c*) Intensity of the bcc (101) diffraction spots. (*d*) Multilayer magnetic moments. The line in (*d*) Represents magnetic moments calculated from bulk moments. Regions I, II, and III, as discussed in the text, are indicated.

explained by elastic strain in the multilayers. The iron layers are under compressive strain, whereas the permalloy layers are under tensile strain. Increasing the Fe thickness relaxes the strain in the Fe layers, and increases the strain on the permalloy layers. This explains the observed change in the in-plane lattice constant.

For $t_{Fe} > 14$ Å the intensity of the fcc diffraction peaks is strongly decreased, and it is not possible to obtain meaningful parameters from fitting these data. At the same time the width of the rocking curves of the (002) specular diffraction spots increases, as depicted in panel (*b*) of fig. 2. This indicates that the fcc structure of the films becomes increasingly disordered for thicker Fe layers. We will show that this is directly correlated to the onset of the formation of bcc Fe. It should be noted that for Fe layer thicknesses below 11 Å the full width at half-maximum (FWHM) of the rocking curves is smaller than 1.5°, establishing the excellent epitaxial quality of the films.

The strong tetragonal distortion of the Fe layers in region I, which leads to a larger interlayer spacing as expected from purely elastic strain, closely resembles the structural behavior found in Fe/Cu(001). There, at thicknesses up to 4 ML, a phase with vertically expanded interlayer distances is found. Detailed LEED investigations revealed a complicated structure of this phase in Fe/Cu(001), involving sinusoidal shifting and vertical buckling of the entire Fe film [1]. The average interlayer distance was found to be 1.87 Å [1]. The Fe interlayer distances which we

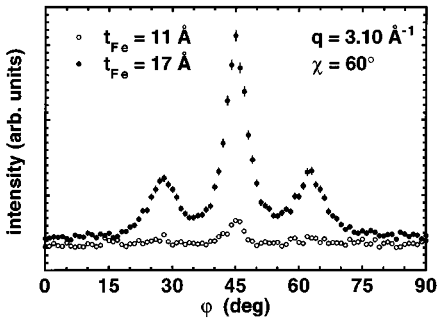

Fig. 3. – Azimuthal scan of the diffracted intensity of $[Ni_{81}Fe_{19}(25\ \text{Å})/Fe(t_{Fe})]_{12}$ multilayers with Fe layer thicknesses $t_{Fe} = 11$ Å (open circles) and 17 Å (filled circles) at a scattering vector $q = 3.10$ Å^{-1}, with angle $\chi = 60°$ to the surface normal.

find in $Fe/Ni_{81}Fe_{19}$ multilayers over the same thickness region (cf. fig. 2 *a*)) match this value. Furthermore the poorer agreement with the simple structural model in region I compared to region II could possibly be accounted for by a complex reconstruction within the Fe layers, perhaps similar to that described in ref. [1]. These authors find a systematic variation of the Fe interlayer spacing away from the Cu(001) substrate. In summary, despite the different environment of the Fe layers in $[Fe/Ni_{81}Fe_{19}(001)]$ and Fe/Cu(001), there is a striking similarity in their structure in region I.

In region II, the simple model used for the fit agrees well with experiment, which indicates a simpler structure for the Fe layers. Taken together with the smaller distortion of 1.4%–3.6%, the Fe structure is a more relaxed fcc structure with respect to region I, similar to that found for Fe films on Cu(001). LEED analysis of Fe/Cu(001) in the thickness range of the relaxed fcc phase of Fe revealed flat Fe atomic planes with no vertical distortion except for the topmost layer at the Fe/vacuum interface, which remains vertically expanded [2]. Again, we conclude that the same structural behavior is found in the multilayers, with the residual vertical expansion of the Fe layers being due to elastic strain induced by the permalloy layers.

We will now focus on the third structural region, region III, beginning at $t_{Fe} = 13$ Å, which is characterized by reduced X-ray scattering intensity and a substantial broadening of the fcc diffraction spots (fig. 2 *b*)). As mentioned before, this is the result of the formation of bcc Fe, whose presence can be tested by X-ray diffraction. The (101) diffraction from bcc Fe (lattice constant 2.87 Å) occurs at a scattering vector of $q = 3.10$ Å^{-1}. The angle χ from the [101] axis to a (001) surface normal and to a (011) surface normal is 45° and 60°, respectively. At an angle $\chi = 45°$ no diffraction of bcc Fe could be observed for any Fe layer thickness and thus no significant amount of (001)-oriented bcc Fe is formed. Several scans were taken in which the azimuthal angle φ is varied, *i.e.* the sample is rotated about its surface normal. Figure 3 shows scans taken at $\chi = 60°$ and $q = 3.10$ Å^{-1} for Fe layer thicknesses of 11 Å (open circles) and 17 Å (filled circles). The peaks at azimuthal angles $\varphi = 28°$ and $\varphi = 62°$ are identified as contributions from bcc Fe, exhibiting a maximum for $q = 3.10$ Å^{-1}, whereas the peak at $\varphi = 45°$ has its maximum value at $q = 3.05$ Å^{-1} and $\chi = 55°$. The latter results from [111] diffraction of the fcc lattice of the multilayer; as the diffraction spots broaden at larger Fe layer thicknesses, the shoulder of these spots becomes more intense in the X-ray scans, as shown in fig. 3.

The bcc diffraction spots at $\varphi = 28°$ and 62° are first observed at Fe layer thicknesses around 11 Å (cf. fig. 3) and increase in intensity with increasing Fe layer thickness. A plot of the intensity of these spots *vs.* Fe layer thickness is given in fig. 2 (*c*). It is obvious that the broadening of the fcc diffraction spots (fig. 2 (*b*)) parallels the increase in bcc diffraction intensity. The decrease in fcc epitaxial quality of the multilayers is thus directly correlated with the appearance of bcc Fe.

The bcc Fe formed in the multilayers is (011) oriented. The same orientation was found in Fe films on Cu(001), where bcc Fe is formed for Fe thicknesses above 10-11 ML [5], [7]. Our X-ray diffraction data show that the projection of the bcc [101] axis onto the surface plane is rotated by 28° with respect to the [100] axis of the fcc material. In Fe/Cu(001), a similar azimuthal orientation of the bcc Fe was observed [7].

We will now focus on the magnetic behavior. Figure 2 (*d*) shows the magnetic moment of the multilayers as a function of Fe layer thickness, measured at room temperature with a commercial SQUID magnetometer. In region I, the moments show an almost linear increase with t_{Fe}, as is expected for an entirely magnetic structure. The solid line in fig. 2 (*d*) represents calculated moments using bulk magnetic moments of iron and permalloy [10]. A pronounced deviation from this linear behavior is observed in region II. The magnetic moment of the multilayers decreases, reaching a minimum at about 12 Å Fe layer thickness with a moment comparable to that at $t_{\mathrm{Fe}} \approx 3.5$ Å. This implies that in the second Fe thickness range a significant amount of Fe exhibits no magnetic moment. In region III, the magnetic moment again strongly increases with increasing Fe thickness, approaching the calculated moments. This can be attributed to the formation of bcc Fe, which, in contrast to the relaxed fcc Fe, shows ferromagnetic behavior.

The finding of non-magnetic iron in region II parallels the magnetic behavior observed for the relaxed fcc phase in Fe/Cu(001). Kerr measurements have shown that in that system the average Fe magnetic moment of the relaxed fcc structure is strongly reduced [3], [5]. This is attributed to an antiferromagnetic phase of Fe, correlated to the structural phase via the atomic volume [8]. Whereas in the expanded phase an atomic volume of 12.1 Å^3 was obtained from a LEED analysis, the Fe in the relaxed phase assumes a volume of 11.4 Å^3 [1], [2]. The atomic volume of Fe in the multilayers ranges from 11.8 Å^3 at $t_{\mathrm{Fe}} = 5$ Å to 11.4 Å^3 at $t_{\mathrm{Fe}} = 13$ Å. The volume expansion of phase I of the multilayers is slightly smaller than that for Fe/Cu(001), but the volume in phase II is identical to that of Fe/Cu(001). We conclude that the reason for the reduced magnetic moment in region II, as in Fe/Cu(001), is the dependence of the magnetic phase of fcc Fe on the lattice constant, as outlined in ref. [8].

In summary, all of the various structural and magnetic phases found in thin (001)-oriented epitaxial Fe films grown on Cu(001) have been reproduced in sputter-deposited epitaxial (001) multilayers where the Fe layers are sandwiched between thin permalloy layers. This clearly shows that the structure of thin Fe is driven by lattice strain induced by the neighboring layers. The use of sputter deposition allows for the study of a wider range of structures than is possible for thin Fe layers grown on metallic single-crystal substrates. In particular, the resistive and magnetoresistive properties of structures containing Fe layers in its different forms can be explored. One of the most interesting of these is the possibility that thin non-magnetic Fe layers could act as "non-magnetic" spacer layers and thus give rise to antiferromagnetic exchange coupling of ferromagnetic layers, and giant magnetoresistance (GMR). This will be the topic of a forthcoming publication.

***

We thank M. F. TONEY for fruitful discussions, and K. P. ROCHE for his technical expertise. SSPP thanks the Office of Naval Research for partial support of this work.

REFERENCES

[1] Müller S., Bayer P., Reischl C., Heinz K., Feldmann B., Zillgen H. and Wuttig M., *Phys. Rev. Lett.*, **74** (1995) 765; Müller S., Bayer P., Kinne A., Reischl C., Metzler R. and Heinz K., *Surf. Sci.*, **331-333** (1995) 723.

[2] Bayer P., Müller S., Schmailzl P. and Heinz K., *Phys. Rev. B*, **48** (1993) 17611.

[3] Li D., Freitag M., Pearson J., Qiu Z. Q. and Bader S. D., *Phys. Rev. Lett.*, **72** (1994) 3112; *J. Appl. Phys.*, **76** (1994) 6425.

[4] Ellerbrock R. D., Fuest A., Schatz A., Keune W. and Brand R. A., *Phys. Rev. Lett.*, **74** (1995) 3053.

[5] Thomassen J., May F., Feldmann B., Wuttig M. and Ibach H., *Phys. Rev. Lett.*, **69** (1992) 3831.

[6] Giergiel J., Kirschner J., Landgraf J., Shen J. and Woltersdorf J., *Surf. Sci.*, **310** (1994) 1.

[7] Schmailzl P., Schmidt K., Bayer P., Döll R. and Heinz K., *Surf. Sci.*, **312** (1994) 73.

[8] Moruzzi V. L., Marcus P. M., Schwartz K. and Mohn P., *Phys. Rev. B*, **34** (1986) 1784; Moruzzi V. L., Marcus P. M. and Kübler J., *Phys. Rev. B*, **39** (1989) 6957.

[9] Fullerton E. E., Schuller I. K., Vanderstraeten H. and Bruynseraede Y., *Phys. Rev. B*, **45** (1992) 9292.

[10] Cullity B. D., *Introduction to Magnetic Materials* (Addison-Wesley, Reading, MA) 1972.